



# Sintering behavior and microwave dielectric properties of $\text{Li}_4\text{Mg}_3[\text{Ti}_{0.8}(\text{Mg}_{1/3}\text{Ta}_{2/3})_{0.2}]_2\text{O}_9$ ceramics with LiF additive for LTCC applications

Z.B. Feng <sup>a</sup>, B.J. Tao <sup>a</sup>, W.F. Wang <sup>a</sup>, H.Y. Liu <sup>a</sup>, H.T. Wu <sup>a,\*</sup>, Z.L. Zhang <sup>b,\*\*</sup>

<sup>a</sup> School of Materials Science and Engineering, University of Jinan, Jinan, 250022, PR China

<sup>b</sup> State Key Laboratory of Biobased Material and Green Papermaking, Qilu University of Technology (Shandong Academy of Sciences), Jinan, 250353, PR China



## ARTICLE INFO

### Article history:

Received 5 September 2019

Received in revised form

29 December 2019

Accepted 31 December 2019

Available online 2 January 2020

### Keywords:

$\text{Li}_4\text{Mg}_3[\text{Ti}_{0.8}(\text{Mg}_{1/3}\text{Ta}_{2/3})_{0.2}]_2\text{O}_9$

LiF

Microwave dielectric properties

LTCC

## ABSTRACT

Novel low temperature sintered  $\text{Li}_4\text{Mg}_3[\text{Ti}_{0.8}(\text{Mg}_{1/3}\text{Ta}_{2/3})_{0.2}]_2\text{O}_9$  ( $\text{LMT}_{0.8}(\text{MT})_{0.2}$ ) ceramics with 1–5 wt% LiF additives were successfully prepared by the solid-state reaction method. The effects of LiF additives on the phase composition, sintering characteristic, microstructure and microwave dielectric properties of  $\text{LMT}_{0.8}(\text{MT})_{0.2}$  ceramics were investigated in detail for the first time. The sintering temperature of  $\text{LMT}_{0.8}(\text{MT})_{0.2}$  ceramics could be effectively lowered to 950 °C by the addition of LiF. A single rock salt crystalline phase structure belonging to a space group of  $\text{Fm}-3\text{m}$  (No.225) was obtained through X-ray diffraction patterns. Dense uniform morphology was observed at 950 °C for  $\text{LMT}_{0.8}(\text{MT})_{0.2}$  ceramics with 3–5 wt% LiF in terms of scanning electron microscopy photographs. Particularly, the  $\text{LMT}_{0.8}(\text{MT})_{0.2}$ –4 wt% LiF ceramics sintered at 950 °C for 4 h possessed optimum microwave dielectric properties of  $\epsilon_r = 16.10$ ,  $Q_f = 114,313$  GHz (at 8.18 GHz) and  $\tau_f = -7.72$  ppm/°C. In addition, the excellent chemical compatibility with silver metal electrodes indicated that the  $\text{LMT}_{0.8}(\text{MT})_{0.2}$ –4 wt% LiF ceramics might be a promising candidate for the low-loss low temperature co-fired ceramics (LTCC) applications in microwave devices.

© 2020 Elsevier B.V. All rights reserved.

## 1. Introduction

As the critical materials of multifunctional electronic components, microwave dielectric materials with superior dielectric properties at microwave frequencies have been considered to play a key role in the field of microwave electronic devices, such as dielectric substrates, resonators, radar, and Internet of Things (IoT), etc. [1–4]. Nowadays, low-temperature co-fired ceramics (LTCC) technology has attracted more and more attention because of the increasing demand of higher miniaturization and integration ability for modern microwave circuit system. However, whether microwave dielectric ceramics could be practically applied in the fabrication of LTCC devices depend upon the following essential requirements: high-permittivity ( $\epsilon_r$ ) values facilitate devices miniaturization, low dielectric-loss (great  $Q_f$ ,  $Q = \tan\delta^{-1}$ ,  $f$ =resonant frequency) values for a good frequency selectivity, near

zero temperature coefficient of resonant frequency ( $\tau_f$ ~0 ppm/°C) values to ensure thermal stabilities, and the internal metallic electrodes (such as Al, Cu, Ag, etc.) could compatible with the studied dielectric materials at relatively low sintering temperatures [5,6]. At present, much more researches were focus on new findings about microwave dielectric ceramic systems [7–10], the improvements on properties by equivalent ion substitution [11–15] and the enhancements on sintering characteristics by adding sintering additives [16–18]. Especially, a great number of dielectric materials with low sintering temperatures, such as  $\text{NaCa}_4\text{V}_5\text{O}_{17}$ ,  $0.35\text{Ag}_2\text{MoO}_4$ – $0.65\text{Ag}_{0.5}\text{Bi}_{0.5}\text{MoO}_4$ ,  $\text{SrMV}_2\text{O}_7$  ( $\text{M} = \text{Mg}, \text{Zn}$ ),  $\text{Li}_{1.6}\text{Zn}_{1.6}\text{Sn}_{2.8}\text{O}_8$  ceramics, etc., might be promising candidates for LTCC applications [19–29].

Recently, it has been found that the new  $\text{Li}_4\text{Mg}_3\text{Ti}_2\text{O}_9$  ceramics with rock salt structure have received enormous attention owing to the excellent microwave dielectric properties ( $\epsilon_r = 15.97$ ,  $Q_f = 135,800$  GHz, and  $\tau_f = -7.06$  ppm/°C) at 1450 °C [30]. Subsequently, the enhancement in dielectric properties of  $\text{Li}_4\text{Mg}_3\text{Ti}_2\text{O}_9$  ceramics were successfully achieved by the partial isovalent complex ions of  $(\text{Mg}_{1/3}\text{Ta}_{2/3})^{4+}$  co-substitution for tetravalent transition metal cations ( $\text{Ti}^{4+}$ ), and the best  $Q_f$  of 160,575 GHz was obtained

\* Corresponding author.

\*\* Corresponding author.

E-mail address: [mse\\_wuht@ujn.edu.cn](mailto:mse_wuht@ujn.edu.cn) (H.T. Wu).

in  $\text{Li}_4\text{Mg}_3[\text{Ti}_{0.8}(\text{Mg}_{1/3}\text{Ta}_{2/3})_{0.2}]_2\text{O}_9$  sample along with  $\epsilon_r = 15.77$  and  $\tau_f = 0 \text{ ppm}/^\circ\text{C}$  when sintered at  $1550^\circ\text{C}$  for 4 h [31]. However, the sintering temperature is too high to satisfy the possible LTCC applications. In general, sintering aid, such as fluoride ( $\text{BaF}_2$ ,  $\text{SrF}_2$ , and  $\text{LiF}$ , etc.), oxides ( $\text{CuO}$ ,  $\text{B}_2\text{O}_3$ ,  $\text{Bi}_2\text{O}_3$ , etc) with low melting points or glass ( $\text{Li}_2\text{O}-\text{B}_2\text{O}_3-\text{SiO}_2$  (LBS),  $\text{ZnO}-\text{B}_2\text{O}_3-\text{SiO}_2$  (ZBS),  $\text{BaCu}(\text{B}_2\text{O}_5)$ , etc.), are added to lower the higher sintering temperature of the matrix materials [32–37]. Among them, lithium fluoride ( $\text{LiF}$ ) is an effective sintering additive to accelerate densification and to lower the sintering temperature of microwave dielectric materials due to its low melting point of  $845^\circ\text{C}$  [32]. For example, Lai et al. lowered the sintering temperature of the  $\text{CaMgSi}_2\text{O}_6$  ceramics with monoclinic structure from  $1250^\circ\text{C}$  to  $900^\circ\text{C}$  with 2 wt%  $\text{LiF}$  [38]. 0.63 $\text{Li}_2\text{Mg}_3\text{SnO}_6$ –0.37 $\text{Ba}_3(\text{VO}_4)_2$  ceramic by using 3 wt%  $\text{LiF}$  sintered at  $850^\circ\text{C}$  for 6 h was reported with good properties of  $\epsilon_r = 12.8$ ,  $Q_f = 101,705 \text{ GHz}$  and  $\tau_f = -2.9 \text{ ppm}/^\circ\text{C}$  [39]. Furthermore, Zhang et al. discovered that 0.85 $\text{Li}_2\text{MgTi}_3\text{O}_8$ –0.15 $\text{LiF}$  ceramics exhibited an excellent combination of microwave dielectric ( $\epsilon_r = 27.8$ ,  $Q_f = 63,000 \text{ GHz}$ , and  $\tau_f = -4.1 \text{ ppm}/^\circ\text{C}$ ) with sintering temperature of  $850^\circ\text{C}$  [40].

To our best knowledge, the influences of  $\text{LiF}$  additives on sintering behavior and microwave dielectric properties of  $\text{LMT}_{0.8}(\text{MT})_{0.2}$  solid solutions have not been reported up to now. Therefore, the improvement in sintering characteristics of  $\text{LMT}_{0.8}(\text{MT})_{0.2}$  ceramics by selecting  $\text{LiF}$  as sintering aid, and the  $\text{LMT}_{0.8}(\text{MT})_{0.2} + x \text{ wt\% LiF}$  samples ( $x = 1$ –5) were prepared successfully through the solid-state route in the present study. The phase purity, sinterability, microstructures, densification, microwave dielectric properties and the chemical compatibility with silver electrode of the novel  $\text{LiF}$ -doped  $\text{LMT}_{0.8}(\text{MT})_{0.2}$  ceramics also were investigated scientifically.

## 2. Experimental procedure

The  $\text{LiF}$ -doped  $\text{LMT}_{0.8}(\text{MT})_{0.2}$  composite ceramics were prepared by solid-state process. High-purity starting materials  $\text{Li}_2\text{CO}_3$  (99.99% metals basis, Aladdin),  $\text{Ta}_2\text{O}_5$  (99.5% metals basis, Aladdin),  $\text{MgO}$  (AR, 98%, Macklin) and  $\text{TiO}_2$  (99.8% metals basis, Macklin) were weighed according to the desired stoichiometric ratio of  $\text{LMT}_{0.8}(\text{MT})_{0.2}$  compounds, and ball-milled using  $\text{ZrO}_2$  balls for 24 h in anhydrous alcohol medium. Then all the dried slurries were calcined at  $1050^\circ\text{C}$  for 2 h to form  $\text{LMT}_{0.8}(\text{MT})_{0.2}$  phase. The powders were re-ground with different quantities (1 wt%, 2 wt%, 3 wt%, 4 wt%, 5 wt%) of  $\text{LiF}$  (99%, Aladdin) for 24 h, and dried at  $80^\circ\text{C}$  once again. Afterwards, 8 wt% paraffin wax as the adhesion agent were added to the obtained mixture powders and then uniaxially pressed into green cylindrical samples with dimension of 10 mm and height of about 6 mm under a pressure of 200 MPa. Finally, these formed  $\text{LMT}_{0.8}(\text{MT})_{0.2} + x \text{ wt\% LiF}$  ( $x = 1, 2, 3, 4$  and 5) pellets were sintered at  $800$ – $1150^\circ\text{C}$  for 4 h in air after all specimens were pretreated at  $500^\circ\text{C}$  for 4 h to remove the organic binder.

The phase constitutions of the sintered  $\text{LMT}_{0.8}(\text{MT})_{0.2} + x \text{ wt\% LiF}$  ( $1 \leq x \leq 5$ ) ceramics were investigated in the 2-theta range from  $30^\circ$  to  $100^\circ$  to collect intensity data by means of X-ray powder diffractometer (XRD, 40 Kv/40 mA) using  $\text{Cu-K}\alpha$  ( $\lambda = 1.542 \text{ \AA}$ ) radiation. The apparent densities ( $\rho_{app}$ ) of as-sintered pellets were measured through liquid Archimedean method. Scanning electron microscopy (SEM, FEI Co., United States) equipped with X-MAX-50 type Energy Dispersive X-ray spectroscopy (EDXS) was employed to analyze the surface micro-structure and chemical compatibility of the sintered specimens. The  $\epsilon_r$  and  $Q_f$  values in microwave frequencies ranging from 8.0 to 12.5 GHz were measured by Hakki–Coleman dielectric resonator method [41] using the N5234A-200 vector network analyzer (Agilent Co., USA) and TE01d shielded cavity method [42], respectively. The  $\tau_f$  (ppm/ $^\circ\text{C}$ ) values

were calculated on the basis of the following equation:

$$\tau_f = \frac{f_{85} - f_{25}}{60 \times f_{25}} \times 10^6 (\text{ppm}/^\circ\text{C}) \quad (1)$$

where,  $f_{85}$  and  $f_{25}$  denoted the resonant frequency at  $85^\circ\text{C}$  and  $25^\circ\text{C}$ , respectively.

## 3. Results and discussion

**Fig. 1** presented the typical room temperature powder XRD diffraction patterns of  $\text{LMT}_{0.8}(\text{MT})_{0.2}$  ceramics with different  $\text{LiF}$  doping contents (1–5 wt%) sintered at different temperatures for 4 h. It is visible from **Fig. 1** that all the diffraction peaks were well indexed to the cubic-type  $\text{LiFeO}_2$  (JCPDS#70-2711) phase structure. And no obvious impure phases were detected in the  $\text{LiF}$ -doped  $\text{LMT}_{0.8}(\text{MT})_{0.2}$  ceramics, which indicated a single rock-salt crystalline phase with a space group Fm-3m (No. 225) in the prepared  $\text{LMT}_{0.8}(\text{MT})_{0.2}$  with  $x \text{ wt\% LiF}$  ( $1 \leq x \leq 5$ ) solid solution samples were successfully formed, which was corresponding to the results reported by Xing et al. [31]. No any  $\text{LiF}$  phase could be obviously detected except for the bottom phase peaks owing to the replacement of larger  $\text{O}^{2-}$  ion (ionic radius of  $1.40 \text{ \AA}$ ) with  $\text{F}^-$  ion (ionic radius of  $1.33 \text{ \AA}$ ), this similar phenomenon also could be found in  $\text{LiF}$ -doped LMS-CST system [43]. Notably, the angle  $2\theta$  position and intensity of the diffraction peaks did not change dramatically with the increase amount of  $\text{LiF}$ , which were considered that the crystal structure of the  $\text{LMT}_{0.8}(\text{MT})_{0.2}$  ceramic matrix [31] did not change by introduction of  $\text{LiF}$  additives.

The variations in apparent densities of  $\text{LMT}_{0.8}(\text{MT})_{0.2-x} \text{ wt\% LiF}$  ( $1 \leq x \leq 5$ ) ceramics as a function of sintering temperatures were shown in **Fig. 2**. The apparent densities of  $\text{LiF}$ -doped  $\text{LMT}_{0.8}(\text{MT})_{0.2}$  ceramics exhibited an upward tendency at first, which was ascribed to the reduction of porosity caused by the formation of liquid phase during the sintering process, and then kept stable when the sintering temperature was further increased. For the  $\text{LMT}_{0.8}(\text{MT})_{0.2}$  samples doped with 3–5 wt%  $\text{LiF}$ , the relatively saturation apparent density value of  $\sim 3.61 \text{ g/cm}^3$  was obtained in the sintering temperature region of  $950^\circ\text{C}$ – $1050^\circ\text{C}$ , which was closed to the apparent density (around  $3.60 \text{ g/cm}^3$ ) of the matrix sintered at  $1550^\circ\text{C}$  for 4 h [31]. Yet, the maximum apparent densities ( $2.93 \text{ g/cm}^3$  for  $x = 1$  and  $3.40 \text{ g/cm}^3$  for  $x = 2$ ) of the samples were lower

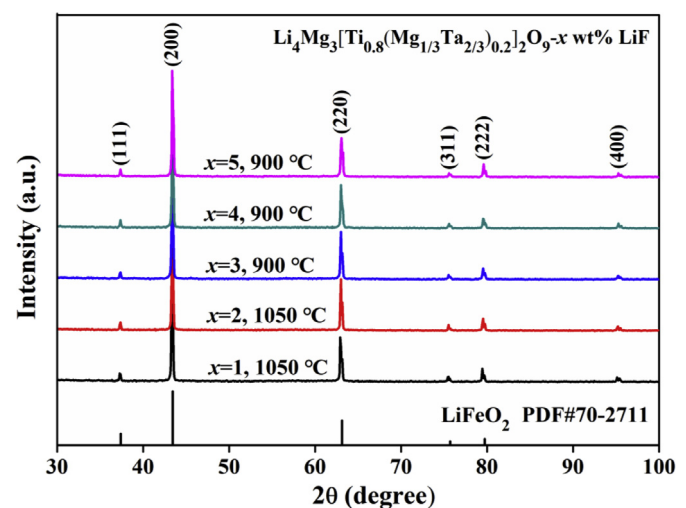


**Fig. 1.** XRD patterns of the  $\text{Li}_4\text{Mg}_3[\text{Ti}_{0.8}(\text{Mg}_{1/3}\text{Ta}_{2/3})_{0.2}]_2\text{O}_9-x \text{ wt\% LiF}$  ( $x = 1$ –5) ceramics sintered at different temperatures for 4 h.

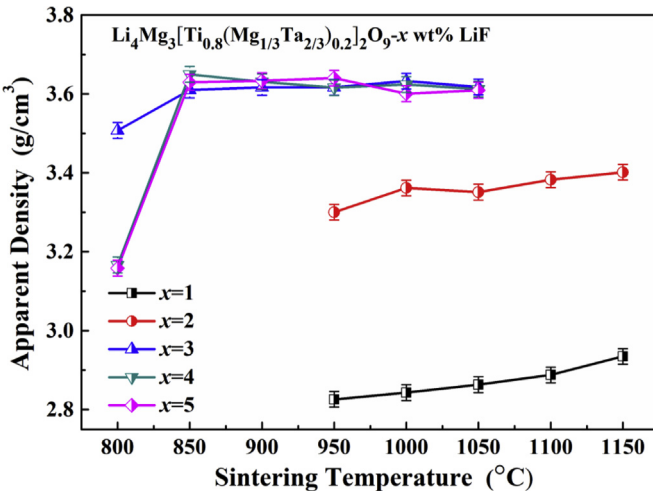


**Fig. 2.** Apparent densities of the  $\text{Li}_4\text{Mg}_3[\text{Ti}_{0.8}(\text{Mg}_{1/3}\text{Ta}_{2/3})_{0.2}]_2\text{O}_{9-x}$  wt% LiF ( $x = 1–5$ ) ceramics as a function of the sintering temperature.

than others, indicating that doping amount of 1–2 wt% LiF was not sufficient to promote the densification process of  $\text{LMT}_{0.8}(\text{MT})_{0.2}$  ceramics and has little contribution to reducing sintering temperature during sintering process. Therefore, it could be proved that adding appropriate LiF as a sintering additive is one of the effective methods for promoting the sintering characteristics of the  $\text{LMT}_{0.8}(\text{MT})_{0.2}$  ceramics at low temperature.

**Fig. 3** illustrated the SEM micrographs of  $\text{LMT}_{0.8}(\text{MT})_{0.2}$ –x wt% ( $1 \leq x \leq 5$ ) LiF ceramics sintered at 950 °C for 4 h. As exhibited in **Fig. 3** (a)–(b), it was clear that some intergranular pores existed on the surface of the sample accompanied by small grain size of approximately 1–2  $\mu\text{m}$ , which indicated that a small amount of liquid phase resulted in the incomplete growth of grains. When 3–5 wt% LiF were added to the samples (**Fig. 3** (c)–(e)), the compactness gradually increased and average grain sizes enlarged above 2  $\mu\text{m}$  as well as more uniform, and the grain boundaries were also well defined, which could be attributed to LiF liquid phase

promoted the growth of grains. Therefore, the moderate LiF addition could obtain a dense and uniform micro-structure with well-packed grains and significantly promote the sintering behaviors of  $\text{LMT}_{0.8}(\text{MT})_{0.2}$  ceramics, which were in accordance with the results of apparent densities.

**Fig. 4** exhibited the curves of dielectric constants ( $\epsilon_r$ ) for  $\text{LMT}_{0.8}(\text{MT})_{0.2}$  ceramics with various LiF doping contents (1–5 wt%) sintered at 800–1150 °C. Generally, the  $\epsilon_r$  values were mainly dependent on the secondary phases, grain boundaries, density and pores etc. extrinsic factors [44]. The formation of pure phase for all LiF-doped  $\text{LMT}_{0.8}(\text{MT})_{0.2}$  ceramics were confirmed through XRD patterns shown in **Fig. 1**. When LiF doping contents were larger than 3 wt%, the relative permittivity varied from 12.81 to 16.20 with the sintering temperature increased from 800 °C to 900 °C, then saturation value was observed in the range of 900 °C–1150 °C. For the  $\text{LMT}_{0.8}(\text{MT})_{0.2}$  specimens doped with 1–2 wt% LiF, the variations in  $\epsilon_r$  values were not remarkable with rising in temperature,

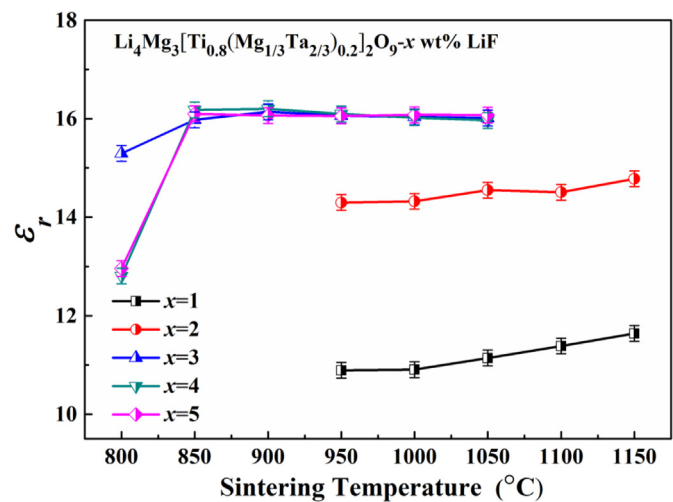


**Fig. 4.** Dielectric constants of  $\text{Li}_4\text{Mg}_3[\text{Ti}_{0.8}(\text{Mg}_{1/3}\text{Ta}_{2/3})_{0.2}]_2\text{O}_{9-x}$  wt% LiF ( $x = 1–5$ ) ceramics sintered at various temperatures.

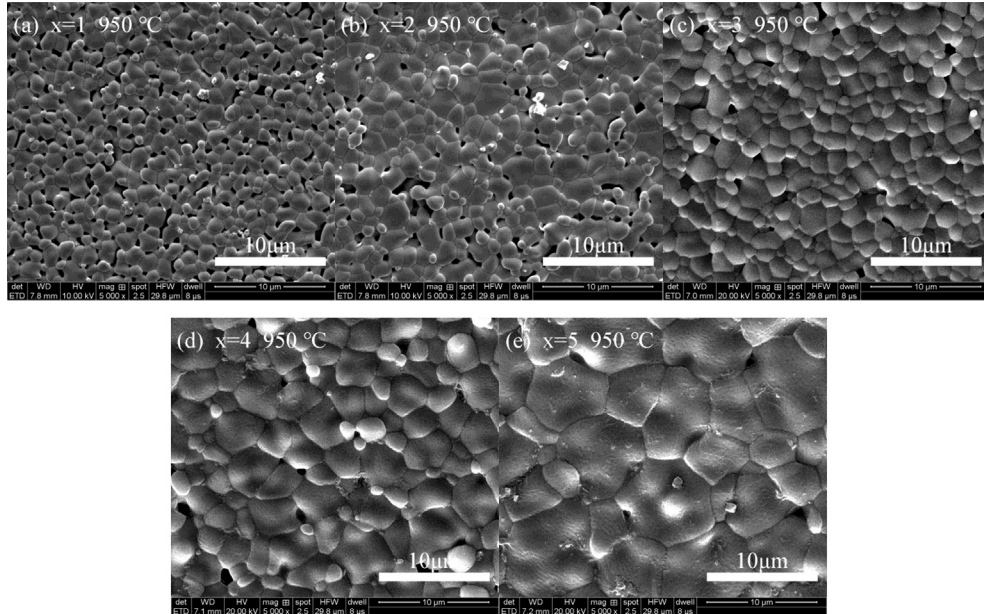


**Fig. 3.** SEM photographs of the obtained  $\text{Li}_4\text{Mg}_3[\text{Ti}_{0.8}(\text{Mg}_{1/3}\text{Ta}_{2/3})_{0.2}]_2\text{O}_{9-x}$  wt% LiF ( $x = 1–5$ ) ceramics sintered at 950 °C for 4 h in air (a–e corresponding to  $x = 1, 2, 3, 4, 5$ ).

and the maximum  $\epsilon_r$  values of 11.64 for  $x = 1$  and of 14.78 for  $x = 2$  all no more than the  $\epsilon_r$  values of above 3 wt% LiF additions, which was ascribed to the porous micro-structure shown in Fig. 3 (a)–(b). It was obvious that the variation in dielectric constant was in good agreement with that of the change tendency in apparent density (Fig. 2). The higher density corresponded to higher dielectric constant, suggesting that density played a major factor in the  $\epsilon_r$  value. In addition, it was worth noting that the  $\epsilon_r$  value (16.10) of the 4 wt% LiF doped LMT<sub>0.8</sub>(MT)<sub>0.2</sub> ceramic densified at 950 °C was quite closed to the  $\epsilon_r$  value (15.77) of the pure LMT<sub>0.8</sub>(MT)<sub>0.2</sub> ceramic sintered at 1550 °C for 4 h [31].

Fig. 5 displayed the quality factors ( $Q_f$ ) of LMT<sub>0.8</sub>(MT)<sub>0.2</sub> samples with various amounts of LiF additives sintered at different temperature. In general, the  $Q_f$  values at the microwave frequencies were greatly affected by both extrinsic factors and intrinsic factors. The extrinsic factors mainly arose from the second phases, compactness, oxygen vacancies, porosity, and grain sizes, while the intrinsic factors involved the structure characteristics and lattice vibration modes [45,46]. The variations of  $Q_f$  had something to do with the extrinsic dielectric loss when lied in a region of lower temperature. The  $Q_f$  values of all the compositions gradually increased with the increase in sintering temperature at first and reached the optimum value, and then slightly declined except the doping amount of 2 wt% when sintering temperature was further increased. Additionally, it was also found that the maximum  $Q_f$  values of 114,313 GHz obtained for LMT<sub>0.8</sub>(MT)<sub>0.2</sub> ceramic by adding 4 wt% LiF was lower than that of previous work [31], which indicated the increase in dielectric loss of the LMT<sub>0.8</sub>(MT)<sub>0.2</sub> samples led by the addition of LiF. Notably, the  $Q_f$  values went up first with the increase of LiF doping, and the subsequent decreased with further increase of LiF content, implying that the quality factor was closely related to the quantity of LiF additive.

The microwave dielectric properties ( $\epsilon_r$ ,  $Q_f$ ,  $\tau_f$ ) of LMT<sub>0.8</sub>(MT)<sub>0.2</sub>-x wt% ( $1 \leq x \leq 5$ ) ceramics sintered at optimum temperature were presented in Fig. 6. The dielectric constant increased from 11.38 at  $x = 1$  to 16.10 at  $x = 3$ , and then stable value was observed at  $x = 3$ –5. Meanwhile, the lower  $Q_f$  values of 22,342 GHz at  $x = 1$  sharply increased to the peak values of 114,313 GHz at  $x = 4$ , then decreased to 103,003 GHz when LiF doping content exceeded 4 wt %. In particular, no obvious change was observed for the measured  $\tau_f$  values with the increase of LiF addition, and varied from -4.54 to -9.32 ppm/°C, suggesting that the amount of LiF additives account for the  $\tau_f$  values. Typically, LMT<sub>0.8</sub>(MT)<sub>0.2</sub> ceramic with 4 wt%

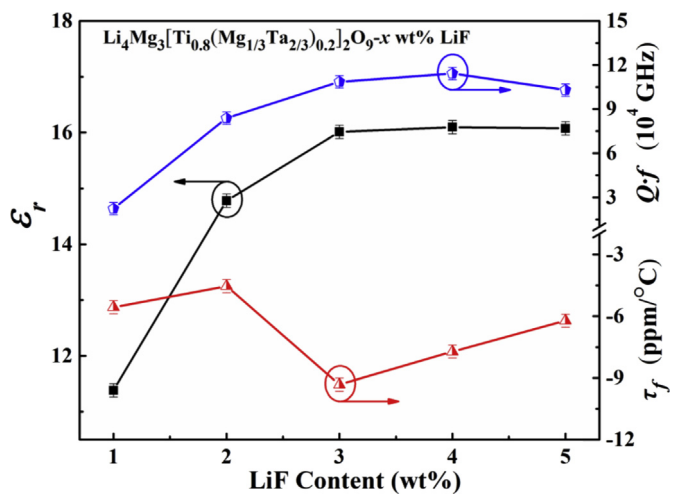


Fig. 6. Microwave dielectric properties of the  $\text{Li}_4\text{Mg}_3[\text{Ti}_{0.8}(\text{Mg}_{1/3}\text{Ta}_{2/3})_{0.2}]_2\text{O}_9$  ceramics doped with 1–5 wt% LiF sintered at optimum temperature.

LiF sintered at 950 °C for 4 h exhibited good microwave dielectric properties of  $\epsilon_r = 16.10$ ,  $Q_f = 114,313$  GHz and  $\tau_f = -7.72$  ppm/°C.

In order to investigate the chemical compatibility with silver (Ag) electrode so that better serve for LTCC applications, XRD patterns of 4 wt% LiF-doped LMT<sub>0.8</sub>(MT)<sub>0.2</sub> ceramic pellet co-fired with 20 wt% Ag powders (99.9%, Macklin, 10 μm) at 950 °C for 4 h were shown in Fig. 7. It was observed that the detectable diffraction patterns corresponded well to the standard card of  $\text{LiFeO}_2$  (JCPDS#70-2711) and of Ag (JCPDS#04-0783), respectively. Besides, no existence of additional peaks in the range of 30–100°, indicating that no any chemical reaction taken place between the Ag and the LMT<sub>0.8</sub>(MT)<sub>0.2</sub>-4 wt% LiF ceramic. In addition, the SEM image of fracture surface and EDXS line scan were performed to analysis the interface between the 4 wt% LiF-doped LMT<sub>0.8</sub>(MT)<sub>0.2</sub> ceramic sheet and the Ag coating co-fired at 950 °C, as shown in Fig. 8(a) and (b). The Ag profile increased sharply on the right side of the boundaries, which suggested that Ag did not spread into zone of LMT<sub>0.8</sub>(MT)<sub>0.2</sub>+x wt% LiF ( $x = 4$ ) ceramics during co-fired. At the same time, this results were also further confirmed by the corresponding EDXS elemental mapping analysis (Fig. 8 (c)–(g)). Hence,

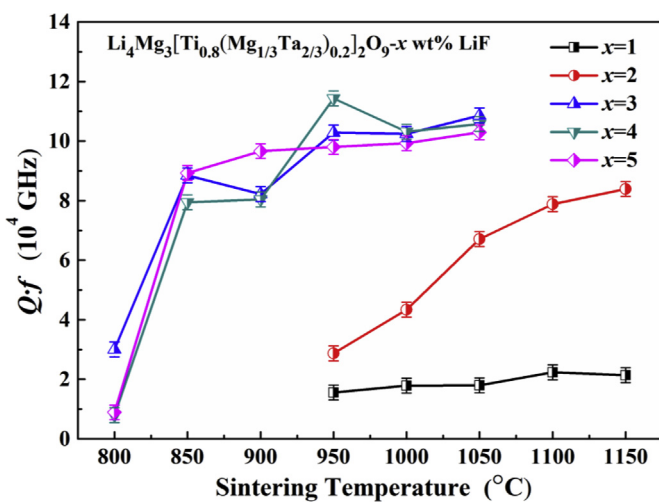


Fig. 5. Quality factors of  $\text{Li}_4\text{Mg}_3[\text{Ti}_{0.8}(\text{Mg}_{1/3}\text{Ta}_{2/3})_{0.2}]_2\text{O}_9$ -x wt% LiF ( $x = 1$ –5) ceramics sintered at various temperatures.

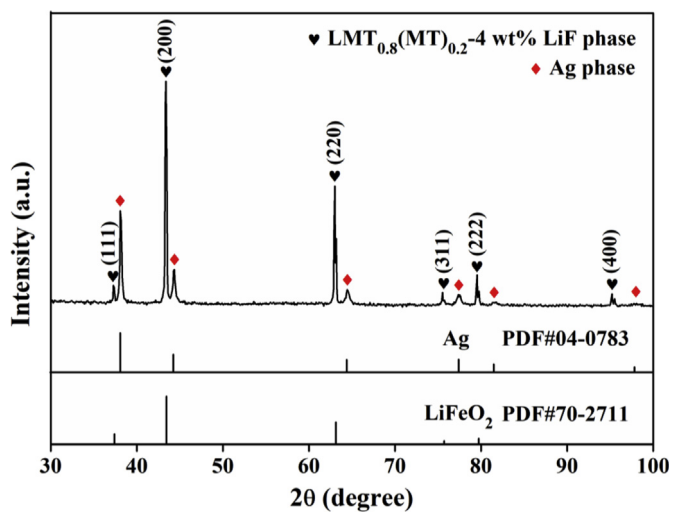
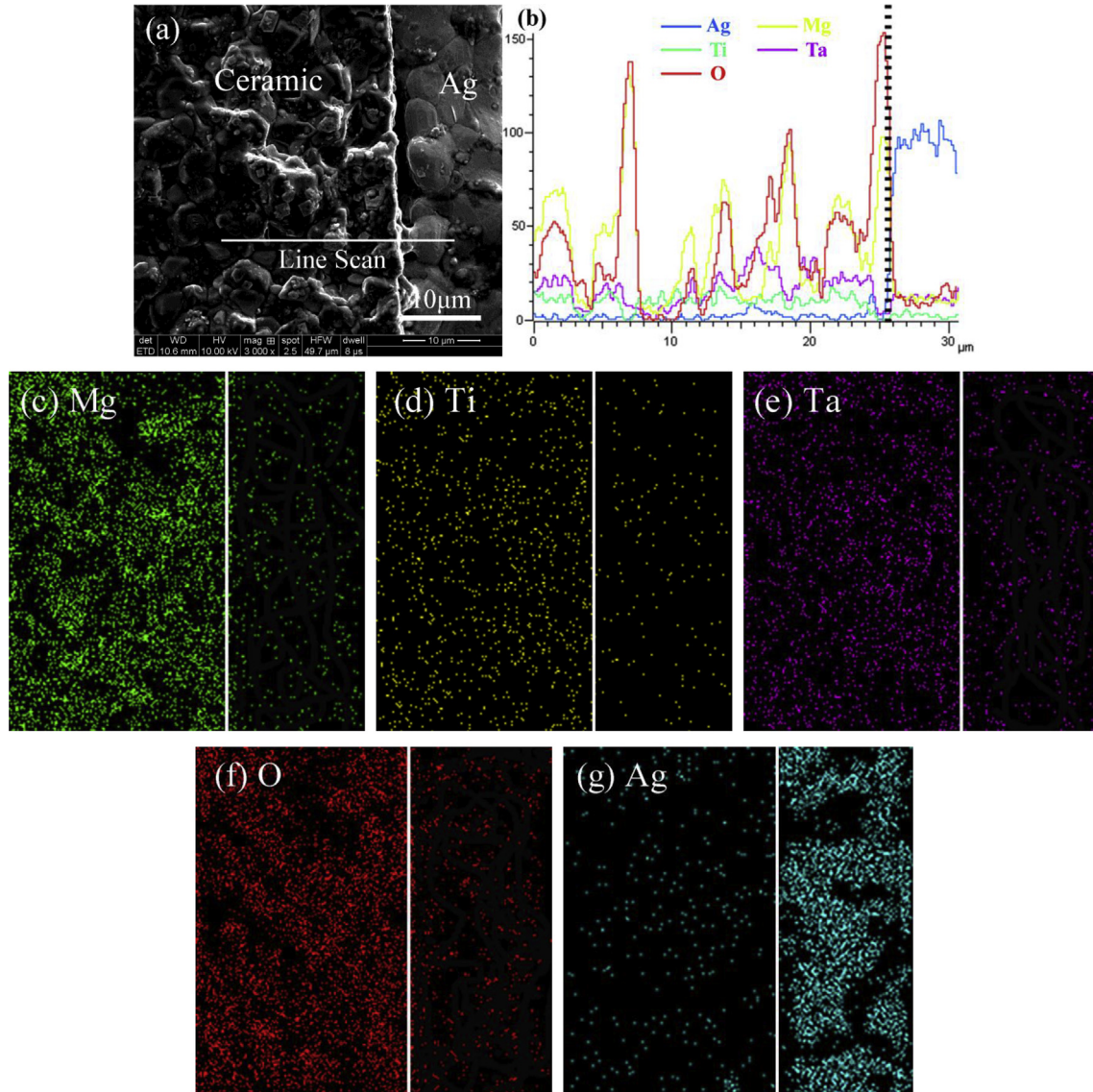


Fig. 7. XRD patterns of  $\text{Li}_4\text{Mg}_3[\text{Ti}_{0.8}(\text{Mg}_{1/3}\text{Ta}_{2/3})_{0.2}]_2\text{O}_9$  doped with 4 wt% LiF mixed with 20 wt% silver powders sintered at 950 °C for 4 h in air.



**Fig. 8.** Typical fractured surface SEM micrograph (a), corresponding EDXS line scanning analysis (b) and EDXS mapping of (c) Mg element, (d) Ti element, (e) Ta element, (f) O element, and (g) Ag element of 4 wt% LiF doped  $\text{Li}_4\text{Mg}_3[\text{Ti}_{0.8}(\text{Mg}_{1/3}\text{Ta}_{2/3})_{0.2}]_2\text{O}_9$  ceramic sheet co-fired with Ag paste at 950 °C for 2 h in air.

the  $\text{LMT}_{0.8}(\text{MT})_{0.2}$ –4 wt% LiF ceramic is a suitable candidate for LTCC applications because of its outstanding microwave dielectric properties and good chemical compatibility with silver electrode.

#### 4. Conclusion

A series of rock-salt structured  $\text{LMT}_{0.8}(\text{MT})_{0.2+x}$  wt% LiF ( $x = 1, 2, 3, 4, 5$ ) ceramics were prepared by the solid-state reaction method at a low temperature. The formation of single crystalline phase with  $\text{Fm}-3\text{m}$  space group in experimental specimens was confirmed by the X-ray diffractometer. The compact samples with 3–5 wt% LiF sintered at 950 °C with homogeneous microstructures were characterized by scanning electron microscopy, indicated the appropriate content of LiF additive could obviously lower the densification sintering temperature of  $\text{LMT}_{0.8}(\text{MT})_{0.2}$  ceramics to a certain extent. The optimal properties with  $\epsilon_r = 16.10$ ,  $Q_f = 114,313$  GHz and  $\tau_f = -7.72$  ppm/°C were achieved in  $\text{LMT}_{0.8}(\text{MT})_{0.2}$  ceramics with 4 wt% LiF sintered at 950 °C. Furthermore, a good chemical compatibility with Ag electrodes

made  $\text{LMT}_{0.8}(\text{MT})_{0.2}$ –4 wt% LiF ceramics as a promising candidate materials for LTCC applications.

#### Declaration of competing interest

The authors declare that they have no known competing financial interests or personal relationships that could have appeared to influence the work reported in this paper.

#### CRediT authorship contribution statement

**Z.B. Feng:** Methodology, Investigation, Data curation, Visualization, Writing - original draft, Writing - review & editing. **B.J. Tao:** Investigation, Validation, Formal analysis. **W.F. Wang:** Methodology, Software, Formal analysis. **H.Y. Liu:** Methodology, Software, Formal analysis. **H.T. Wu:** Conceptualization, Resources, Writing - review & editing, Project administration, Supervision, Funding acquisition. **Z.L. Zhang:** Conceptualization, Resources, Writing - review & editing, Project administration, Supervision, Funding

acquisition.

## Acknowledgements

This work was supported by the National Natural Science Foundation of China (No. 51972143). The authors are thankful to the help of Professor Zhen Xing Yue and postdoctoral Jie Zhang on the measurement of microwave properties in Tsinghua University.

## References

- [1] L.X. Pang, D. Zhou, Modification of NdNbO<sub>4</sub> microwave dielectric ceramic by Bi substitutions, *J. Am. Ceram. Soc.* 102 (2019) 2278–2282.
- [2] Y. Tang, M.Y. Xu, L. Duan, J.Q. Chen, C.C. Li, H.C. Xiang, L. Fang, Structure, microwave dielectric properties, and infrared reflectivity spectrum of olivine type Ca<sub>2</sub>GeO<sub>4</sub> ceramic, *J. Eur. Ceram. Soc.* 39 (2019) 2354–2359.
- [3] Y.H. Zhang, J.J. Sun, N. Dai, Z.C. Wu, H.T. Wu, C.H. Yang, Crystal structure, infrared spectra and microwave dielectric properties of novel extra low-temperature fired Eu<sub>2</sub>Zr<sub>3</sub>(MoO<sub>4</sub>)<sub>9</sub> ceramics, *J. Eur. Ceram. Soc.* 39 (2019) 1127–1131.
- [4] C.X. Su, L. Fang, Z.H. Wei, X.J. Kuang, H. Zhang, LiCa<sub>3</sub>ZnV<sub>3</sub>O<sub>12</sub>: a novel low-firing, high Q microwave dielectric ceramic, *Ceram. Int.* 40 (2014) 5015–5018.
- [5] D. Zhou, L.X. Pang, D.W. Wang, C. Li, B.B. Jin, I.M. Reaney, High permittivity and low loss microwave dielectrics suitable for 5G resonators and low temperature co-fired ceramic architecture, *J. Mater. Chem. C.* 5 (2017) 10094–10098.
- [6] J.X. Bi, C.F. Xing, C.H. Yang, H.T. Wu, Phase composition, microstructure and microwave dielectric properties of rock salt structured Li<sub>2</sub>ZrO<sub>3</sub>-MgO ceramics, *J. Eur. Ceram. Soc.* 38 (2018) 3840–3846.
- [7] P.B. Jiang, Y.D. Hu, S.X. Bao, J. Chen, Z.Z. Duan, T. Hong, C.H. Wu, G. Wang, A novel microwave dielectric ceramic Li<sub>2</sub>NiZrO<sub>4</sub> with rock salt structure, *RSC Adv.* 9 (2019) 32936–32939.
- [8] Z.W. Zhang, L. Fang, H.C. Xiang, M.Y. Xu, Y. Tang, H. Jantunen, C.C. Li, Structural, infrared reflectivity spectra and microwave dielectric properties of the Li<sub>7</sub>Ti<sub>3</sub>O<sub>9</sub>F ceramic, *Ceram. Int.* 45 (2019) 10163–10169.
- [9] C.C. Li, H.C. Xiang, M.Y. Xu, Y. Tang, L. Fang, Li<sub>2</sub>AgO<sub>4</sub> (A=Zn, Mg): two novel low-permittivity microwave dielectric ceramics with olivine structure, *J. Eur. Ceram. Soc.* 38 (2018) 1524–1528.
- [10] M.J. Wu, Y.C. Zhang, M.Q. Xiang, Synthesis, characterization and dielectric properties of a novel temperature stable (1-x)CoTiNb<sub>2</sub>O<sub>8</sub>-xZnNb<sub>2</sub>O<sub>6</sub> ceramic, *J. Adv. Ceram.* 8 (2019) 228–237.
- [11] H.C. Yang, S.R. Zhang, H.Y. Yang, Y. Yuan, E.Z. Li, Influence of (Al<sub>1/3</sub>W<sub>2/3</sub>)<sup>5+</sup> co-substitution for Nb<sup>5+</sup> in NdNbO<sub>4</sub> and the impact on the crystal structure and microwave dielectric properties, *Dalton Trans.* 44 (2018) 15808–15815.
- [12] K. Cheng, C.C. Li, C.Z. Yin, Y. Tang, Y.H. Sun, L. Fang, Effects of Sr<sup>2+</sup> substitution on the crystal structure, Raman spectra, bond valence and microwave dielectric properties of Ba<sub>3-x</sub>Sr<sub>x</sub>(VO<sub>4</sub>)<sub>2</sub> solid solutions, *J. Eur. Ceram. Soc.* 39 (2019) 3738–3743.
- [13] H.H. Guo, D. Zhou, W.F. Liu, L.X. Pang, D.W. Wang, J.Z. Su, Z.M. Qi, Microwave dielectric properties of temperature-stable zircon-type (Bi, Ce)VO<sub>4</sub> solid solution ceramics, *J. Am. Ceram. Soc.* 103 (2020) 423–431.
- [14] Y.H. Zhang, H.T. Wu, Crystal structure and microwave dielectric properties of La<sub>2</sub>(Zr<sub>1-x</sub>Ti<sub>x</sub>)<sub>3</sub>(MoO<sub>4</sub>)<sub>9</sub> (0≤x≤0.1) ceramics, *J. Am. Ceram. Soc.* 102 (2019) 4092–4102.
- [15] X.L. Chen, X. Li, H.F. Zhou, J. Sun, X.X. Li, X. Yan, C.C. Sun, J.P. Shi, Phase evolution, microstructure, electric properties of (Ba<sub>1-x</sub>Bi<sub>0.67x</sub>Na<sub>0.33x</sub>)(Ti<sub>1-x</sub>Bi<sub>0.33x</sub>Sn<sub>0.67x</sub>)O<sub>3</sub> ceramics, *J. Adv. Ceram.* 8 (2019) 427–437.
- [16] X.K. Lan, J. Li, F. Wang, X.H. Wang, W.Z. Lu, M.Z. Hu, W. Lei, A novel low-permittivity LiAl<sub>0.98</sub>(Zn<sub>0.5</sub>Si<sub>0.5</sub>)<sub>0.02</sub>O<sub>2</sub>-based microwave dielectric ceramics for LTCC application, *Int. J. Appl. Ceram. Technol.* (2019), <https://doi.org/10.1111/ijac.13368>.
- [17] T.Y. Qin, C.W. Zhong, Y. Qin, B. Tang, S.R. Zhang, Low-temperature sintering mechanism and microwave dielectric properties of ZnAl<sub>2</sub>O<sub>4</sub>-LMZBS composites, *J. Alloy. Comp.* 797 (2019) 744–753.
- [18] X.L. Shi, H.W. Zhang, D.N. Zhang, F. Xu, G. Wang, Y.H. Zheng, C. Liu, J. Li, L.C. Jin, L.J. Jia, Temperature stability and chemical compatibility of novel Li<sub>1.6</sub>Z<sub>n<sub>1.6</sub></sub>Sn<sub>2.8</sub>O<sub>8</sub> ceramics, *Mater. Chem. Phys.* 238 (2019) 121960.
- [19] C.Z. Yin, C.C. Li, G.J. Yang, L. Fang, Y.H. Yuan, L.L. Shu, J.B. Khalil, NaCa<sub>4</sub>V<sub>5</sub>O<sub>17</sub>: a low-firing microwave dielectric ceramic with low permittivity and chemical compatibility with silver for LTCC applications, *J. Eur. Ceram. Soc.* 40 (2020) 386–390.
- [20] X. Xue, X.F. Yuan, R. Ma, Q.B. Yuan, H. Wang, Temperature stable 0.35Ag<sub>2</sub>MoO<sub>4</sub>-0.65Ag<sub>0.5</sub>Bi<sub>0.5</sub>MoO<sub>4</sub> microwave dielectric ceramics with ultra-low sintering temperatures, *J. Eur. Ceram. Soc.* 39 (2019) 3744–3748.
- [21] E.K. Suresh, R. Ratheesh, Structure and microwave dielectric properties of glass free low temperature co-firable SrMV<sub>2</sub>O<sub>7</sub> (M=Mg, Zn) ceramics, *J. Alloy. Comp.* 808 (2019) 151641.
- [22] H.C. Xiang, L. Fang, W.S. Fang, Y. Tang, C.C. Li, A novel low-firing microwave dielectric ceramic Li<sub>2</sub>ZnGe<sub>3</sub>O<sub>8</sub> with cubic spinel structure, *J. Eur. Ceram. Soc.* 37 (2017) 625–629.
- [23] Z.F. Fu, J.L. Ma, C. Li, H.Y. Fan, P. Liu, Low-fired Li<sub>2</sub>Mg<sub>3</sub>ZrO<sub>6</sub>-based composite ceramics with temperature-stable for LTCC applications, *J. Alloy. Comp.* 812 (2020) 152001.
- [24] H.C. Xiang, C.C. Li, H.L. Jantunen, L. Fang, A.E. Hill, Ultralow loss CaMgGeO<sub>4</sub> microwave dielectric ceramic and its chemical compatibility with silver electrodes for low-temperature cofired ceramic applications, *ACS Sustain. Chem. Eng.* 6 (2018) 6458–6466.
- [25] J.Q. Ren, K. Bi, X.L. Fu, Z.J. Peng, Novel Al<sub>2</sub>Mo<sub>3</sub>O<sub>12</sub>-based temperature-stable microwave dielectric ceramics for LTCC applications, *J. Mater. Chem. C.* 6 (2018) 11465–11470.
- [26] Z.F. Fu, C. Li, J.L. Ma, Y.L. Wu, Low temperature sintering mechanism for Li<sub>2</sub>Mg<sub>3</sub>SnO<sub>6</sub> microwave dielectric ceramics, *Mater. Sci. Eng. B* 250 (2019) 114438.
- [27] K.G. Wang, H.F. Zhou, X.B. Liu, W.D. Sun, X.L. Chen, H. Ruan, A lithium aluminium borate composite microwave dielectric ceramic with low permittivity, near-zero shrinkage, and low sintering temperature, *J. Eur. Ceram. Soc.* 39 (2019) 1122–1126.
- [28] H.H. Guo, D. Zhou, L.X. Pang, Z.M. Qi, Microwave dielectric properties of low firing temperature stable scheelite structured (Ca, Bi)(Mo, V)O<sub>4</sub> solid solution ceramics for LTCC applications, *J. Eur. Ceram. Soc.* 39 (2019) 2365–2373.
- [29] J. Li, L. Fang, H. Luo, J.B. Khalil, Y. Tang, C.C. Li, Li<sub>4</sub>WO<sub>5</sub>: a temperature stable low-firing microwave dielectric ceramic with rock salt structure, *J. Eur. Ceram. Soc.* 36 (2016) 243–246.
- [30] J.X. Bi, Y.J. Niu, H.T. Wu, Li<sub>4</sub>Mg<sub>3</sub>Ti<sub>2</sub>O<sub>9</sub>: a novel low-loss microwave dielectric ceramic for LTCC, *Ceram. Int.* 43 (2017) 7522–7530.
- [31] C.F. Xing, H.T. Wu, Crystal structure and microwave dielectric properties of Li<sub>4</sub>Mg<sub>3</sub>[Ti<sub>1-x</sub>(Mg<sub>1/3</sub>Ta<sub>2/3</sub>)<sub>x</sub>]O<sub>9</sub> (x=0–0.4) ceramics, *Ceram. Int.* 45 (2019) 4142–4145.
- [32] X.Q. Song, K. Du, J. Li, X.K. Lan, W.Z. Lu, X.H. Wang, W. Lei, Low-fired fluoride microwave dielectric ceramics with low dielectric loss, *Ceram. Int.* 45 (2019) 279–286.
- [33] X.Q. Song, W. Lei, Y.Y. Zhou, T. Chen, S.W. Ta, Z.X. Fu, W.Z. Lu, Ultra-low fired fluoride composite microwave dielectric ceramics and their application for BaCuSi<sub>2</sub>O<sub>6</sub>-based LTCC, *J. Am. Ceram. Soc.* 103 (2020) 1140–1148.
- [34] C.Z. Yin, H.C. Xiang, C.C. Li, H. Porwal, L. Fang, Low-temperature sintering and thermal stability of Li<sub>2</sub>GeO<sub>3</sub>-based microwave dielectric ceramics with low permittivity, *J. Am. Ceram. Soc.* 101 (2018) 4608–4614.
- [35] P. Zhang, M.M. Yang, H. Xie, M. Xiao, Z.T. Zheng, Sintering behavior and microwave dielectric properties of low-loss Li<sub>2</sub>Mg<sub>3</sub>Ti<sub>2</sub>O<sub>6</sub> ceramics doped with different glass agents, *Mater. Chem. Phys.* 227 (2019) 130–133.
- [36] H.F. Zhou, X.H. Tan, K.G. Wang, W.D. Sun, H. Ruan, X.L. Chen, Microstructure and sintering behavior of low temperature cofired Li<sub>4/5</sub>Mg<sub>4/5</sub>Ti<sub>7/5</sub>O<sub>4</sub> ceramics containing BaCu(B<sub>2</sub>O<sub>5</sub>) and TiO<sub>2</sub> and their compatibility with a silver electrode, *RSC Adv.* 71 (2017) 44706–44711.
- [37] H.I. Hsiang, C.C. Chen, S.Y. Yang, Microwave dielectric properties of Ca<sub>0.7</sub>N<sub>d</sub>Q<sub>2</sub>TiO<sub>3</sub> ceramic-filled Ca<sub>0.8</sub>B<sub>2</sub>O<sub>3</sub>SiO<sub>2</sub> glass for LTCC applications, *J. Adv. Ceram.* 8 (2019) 345–351.
- [38] Y.M. Lai, H. Su, G. Wang, X.L. Tang, X. Huang, X.F. Liang, H.W. Zhang, Y.X. Li, K. Huang, X.R. Wang, Low-temperature sintering of microwave ceramics with high Q' values through LiF addition, *J. Am. Ceram. Soc.* 102 (2019) 1893–1903.
- [39] J. Zhang, R.Z. Zuo, J. Song, Y.D. Xu, M. Shi, Low-loss and low-temperature firable Li<sub>2</sub>Mg<sub>3</sub>SnO<sub>6</sub>-Ba<sub>3</sub>(VO<sub>4</sub>)<sub>2</sub> microwave dielectric ceramics for LTCC applications, *Ceram. Int.* 44 (2018) 2606–2610.
- [40] X.H. Zhang, Y.M. Ding, J.J. Bian, Sintering behavior, microstructure and microwave dielectric properties of Li<sub>2</sub>MgTi<sub>3</sub>O<sub>8</sub> modified by LiF, *J. Mater. Sci. Mater. Electron.* 28 (2017) 12755–12760.
- [41] B.W. Hakki, P.D. Coleman, A dielectric resonator method of Measuring Inductive capacities in the millimeter range, *IEEE Trans. Microw. Theory Tech.* 8 (1960) 402–410.
- [42] W.E. Courtney, Analysis and evaluation of a method of measuring the complex permittivity and permeability microwave insulators, *IEEE Trans. Microw. Theory Tech.* 18 (1970) 476–485.
- [43] Z.F. Fu, J.L. Ma, P. Liu, Novel temperature stable and low-fired Li<sub>2</sub>Mg<sub>3</sub>SnO<sub>6</sub>-Ca<sub>0.9</sub>Sr<sub>0.1</sub>TiO<sub>3</sub> composite ceramics, *J. Alloy. Comp.* 752 (2018) 354–358.
- [44] L. Fang, Z.H. Wei, C.X. Su, F. Xiang, H. Zhang, Novel low-firing microwave dielectric ceramics: BaMV<sub>2</sub>O<sub>7</sub> (M=Mg, Zn), *Ceram. Int.* 40 (2014) 16835–16839.
- [45] A. Manan, Z. Ullah, A.S. Ahmad, A. Ullah, D.F. Khan, A. Hussain, M.U. Khan, Phase microstructure evaluation and microwave dielectric properties of (1-x) Mg<sub>0.95</sub>Ni<sub>0.05</sub>Ti<sub>0.98</sub>Zr<sub>0.02</sub>O<sub>3</sub>-xCa<sub>0.6</sub>La<sub>0.8/3</sub>TiO<sub>3</sub> ceramics, *J. Adv. Ceram.* 7 (2018) 72–78.
- [46] L. Fang, C.X. Su, H.F. Zhou, Z.H. Wei, H. Zhang, Novel low-firing microwave dielectric ceramic Li<sub>2</sub>Ca<sub>3</sub>MgV<sub>3</sub>O<sub>12</sub> with low dielectric loss, *J. Am. Ceram. Soc.* 96 (2013) 688–690.